Life Sciences 234 (2019) 116739

Contents lists available at ScienceDirect

Life Sciences

journal homepage: www.elsevier.com/locate/lifescie

Icariin improves the cognitive function of APP/PS1 mice via suppressing endoplasmic reticulum stress

Fei Li*, Yangyang Zhang, Xiaofeng Lu, Jingshan Shi, Qihai Gong

Key Laboratory of Basic Pharmacology of Ministry of Education, Joint International Research Laboratory of Ethnomedicine of Ministry of Education, Zunyi Medical University, Zunyi, Guizhou, China

ARTICLE INFO

Keywords:
Icariin
Behavior
Apoptosis
Endoplasmic reticulum stress
Alzheimer's disease

ABSTRACT

Aim: This study aimed to investigate the effect of icariin (referred as ICA) on Alzheimer's disease (AD) model through endoplasmic reticulum (ER) stress pathway.

Main methods: Nine months male APP/PS1 and wild-type (WT) mice were randomly divided into four groups: APP/PS1 control, APP/PS1 + ICA, WT control and WT + ICA groups. The treated mice were given ICA 60 mg/kg/d and control mice were received the same volume distilled water for consecutive 3 months. The Morris water maze and Novel object recognition were used to detect animals' behavior. Nissl staining was used to observe the neuronal morphology in hippocampus area. Aβ deposition in hippocampal region was observed by immunofluorescence staining. TUNEL staining was used to observe apoptosis. Detection of expression of ER stress related factors by Western blot and real time RT-PCR.

Key findings: Chronically administrated with ICA compared with APP/PS1 control mice significantly improved the behavior performance, reduced neuronal apoptosis, as well as suppressing the ER stress signaling pathway, including that decreased the level of glucose-regulated protein 78, phosphorylated ER-regulated kinase and phosphorylated eukaryotic initiation factor α, as well activating transcription factor-4, C/EBP homologous protein, DNA damage inducible protein 34 and tribbles homologous protein 3.

Significance: Our data indicated that ICA suppressed the ER stress signaling to protect against AD animal model, these findings suggest that a potential point for researching the effect of ICA on neurodegeneration.

1. Introduction

Alzheimer's disease (AD) is a devastating neurodegenerative disorder affecting about 50 million people worldwide, and the number of patients will increase exponentially every 20 years according to the 2018 World Alzheimer Report [1]. AD is characterized by a cascade of pathological events, including β-amyloid polypeptide (Aβ) deposition, hyperphosphorylated tau aggregation, synapses and neurons loss, neuroinflammation. $A\beta_{40/42}$ is generated by the sequential cleavage of amyloid precursor protein (APP) by two proteases which, respectively, are β-secretase (β-site APP-cleaving enzyme 1, BACE1) and γ-secretase. Emerging evidence suggests that endoplasmic reticulum (ER) stress induced by exogenous, abnormal misfolded proteins or intracellular calcium imbalance contributing to the salient pathology associated with neurodegeneration [2]. ER is the site of folding for all membrane and secreted proteins, transgenic overexpression of the transmembrane proteins APP can cause ER stress. The glucose-regulated protein 78 (GRP78), possesses both a chaperone and a stress-sensing function, helps fold new proteins in the ER and interacts with the ER stress sensors protein kinase RNA-like ER kinase (PERK), inositol-requiring protein-1 (IRE1), and activating transcription factor-6 (ATF6), preventing their activation. Under stress condition, GRP78 releases these sensors, which then dimerize and auto-phosphorylate (PERK and IRE1) resulting in up-regulation of the transcription factors activating transcription factor-4 (ATF4), C/EBP homologous protein (CHOP), and spliced form of X-box binding protein 1 (XBP1s), which induce the expression of genes involved in ER-associated degradation, antioxidant responses, and apoptosis; or cleave ATF6 in Golgi releasing ATF6 fragment (ATF6f), which translocate to the nucleus and activates transcription of chaperones to help manage the unfolded protein burden [3]. However, chronic and irreversible ER stress results in apoptosis, which plays an important role in many diseases, such as diabetes, neurodegenerative diseases [4]. Some research showed that ER stress is prevalent in AD brain, and then ER stress induced apoptosis is regarded as the possible cause of AD [5,6]. Therefore, suppressing chronic ER stress maybe retard the development or progression of AD.

* Corresponding author at: No.6 West Xuefu Road, Xinpu District, Zunyi City 563006, China.
E-mail address: lifei@zmu.edu.cn (F. Li).

https://doi.org/10.1016/j.lfs.2019.116739
Received 21 March 2019; Received in revised form 30 July 2019; Accepted 5 August 2019
Available online 07 August 2019

Table 1
Specific qPCR primers used in this study.

Gene	Gene ID	Forward primer	Reverse primer
GADD34	NM_008654.2	GGAGGTGGTGGCTAGAGAAGAGG	CGGAGCTATGGAAGCAGCAGAAG
ERO1α	NM_015774.3	GACTGTGTTGGCTGCTTCAA	CCGTCCTCCTCAGTGAACAT
TRB3	NM_175093.2	ACTTGGCTGTGGGATTCAAG	GACTGTGGGCCTGGGTACTA
β-actin	NM_031144.3	GGCCAACCGTGAAAAGATGA	CAGCCTGGATGGCTACGTACA

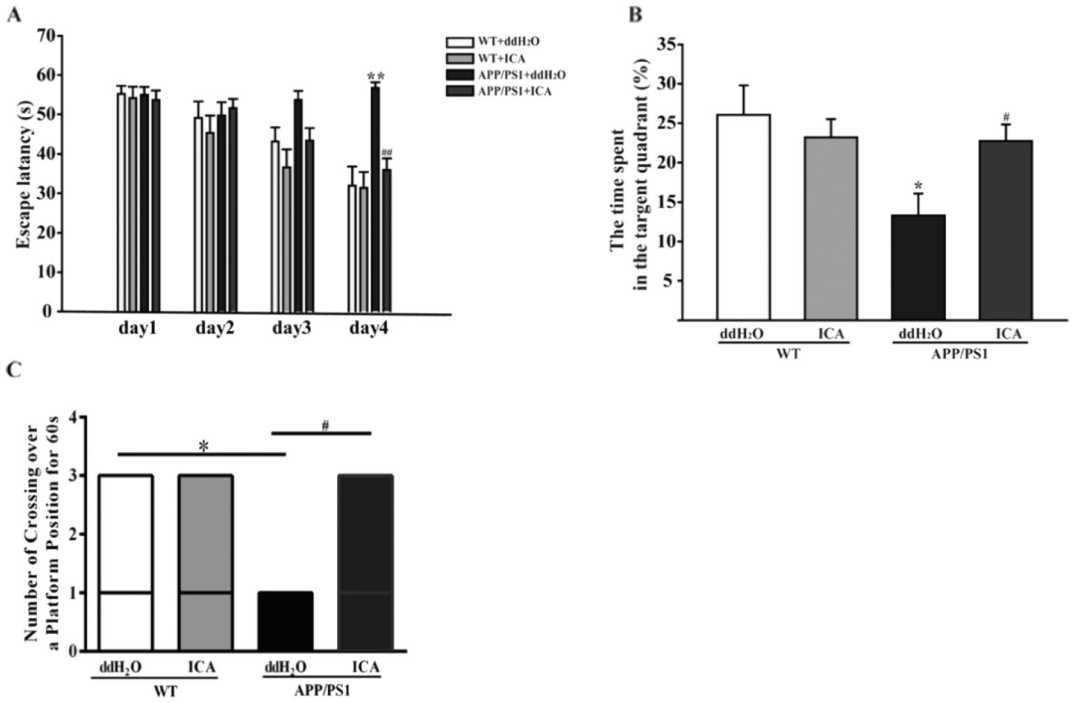

Fig. 1. Effect of ICA on the learning and memory function of APP/PS1 transgenic mice by Morris water maze. (A) The escape latency spent to find the hidden platform from day 1 to day 4. The daily training results were measured by repeated data, followed by Bonferroni multiple comparison tests. The escape latency was gradually shorten as daily training process [$F_{(2.595,134.927)} = 24.372$, $P < 0.001$]. There was significant difference of the escape latency in these four groups [$F_{(3,52)} = 4.069$, $P = 0.011$], in which the escape latency of APP/PS1 group was the longest, ICA treatment significant decreased the time spent to reach the platform. (B) There was alteration in the percent of time that mice swam in the target quadrant [$F_{(3,52)} = 3.869$, $P = 0.014$]. (C) The number of Crossing over the Platform Position within 60 s was follow Kruskal-Wallis H test, there was significant changes between APP/PS1 vs control groups, ICA treated mice vs APP/PS1 mice [$\chi^2_{(3)} = 10.074$, $P = 0.018$]. Note: values were expressed as mean ± S.E.M, $^*P < 0.05$, $^{**}P < 0.01$ vs. WT, $^{\#}P < 0.05$, $^{\#\#}P < 0.01$vs. APP/PS1.

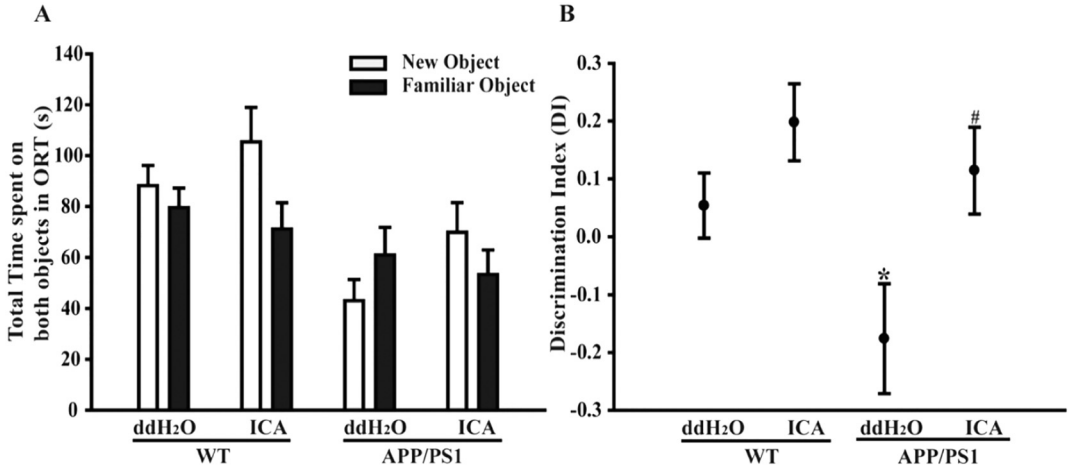

Fig. 2. Effect of ICA on learning and memory function of APP/PS1 transgenic mice by new object recognition assay. (A) Comparison between new object and old object time in mouse recognition, (B) there were differences in mice recognition of new objects and indices of old objects [$F_{(3,52)} = 4.567$, $P = 0.006$]. Note: values were expressed as mean ± S.E.M, $^*P < 0.05$ vs WT + ddH_2O, $^{\#}P < 0.05$ vs APP/PS1 + ddH_2O.

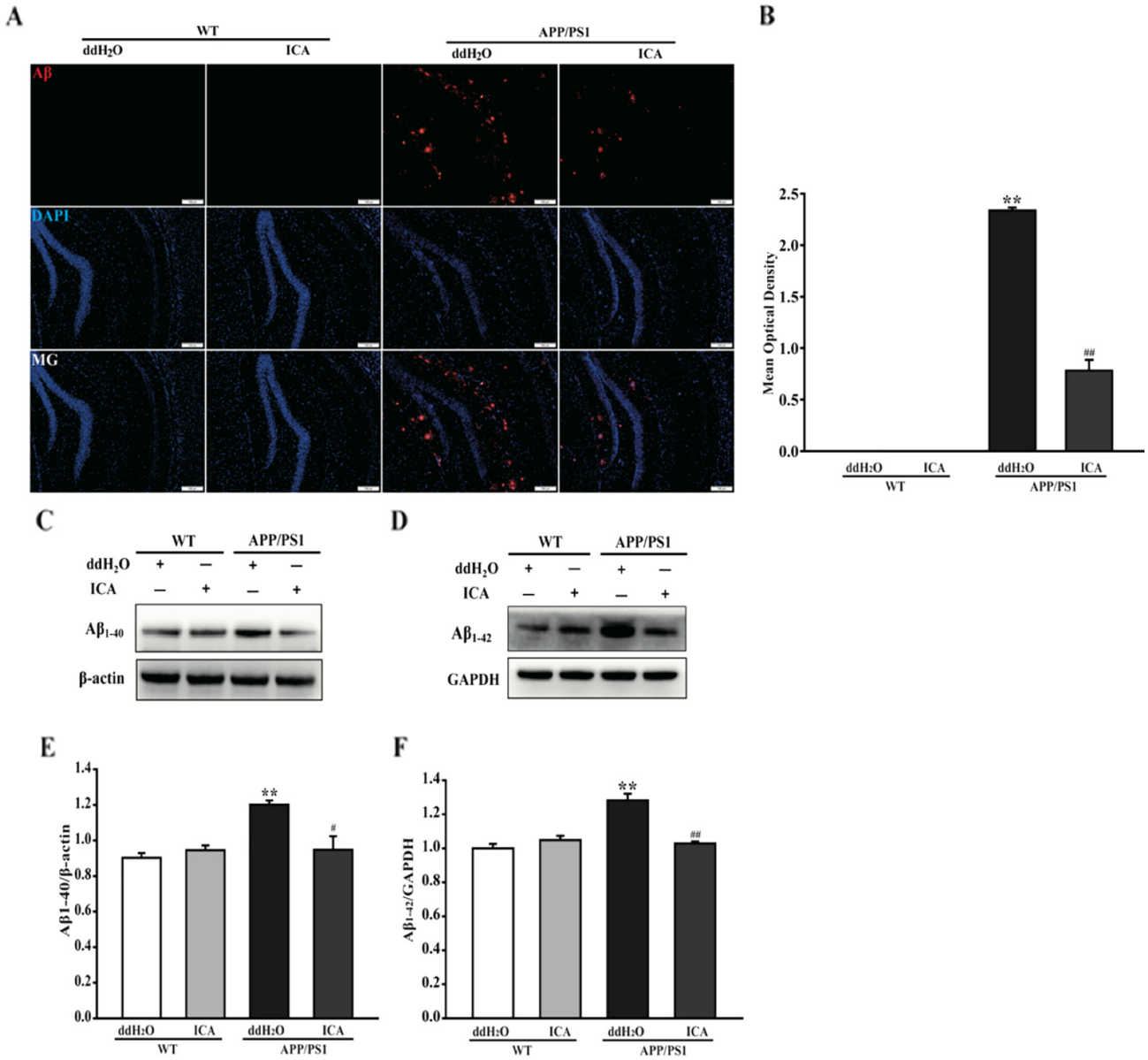

Fig. 3. Effects of ICA on Aβ burden in the hippocampus of APP/PS1 mice. (A) Aβ deposition of hippocampal DG sections by IFC staining (magnification 100×, scale bar 100 μm). (B) Quantitative analysis of the mean optical density of Aβ, as no Aβ positive IFC staining was found in WT control and WT + ICA mice, the difference between APP/PS1 and APP/PS1 + ICA mice was tested by independent samples *t*-test, the results showed that ICA treatment significant Aβ burden [$t_{(6)} = 14.696$, $P < 0.001$]. (C and D) The bands of $A\beta_{1-40}$ and $A\beta_{1-42}$ were observed by Western blot. (E) Quantitative analysis of $A\beta_{1-40}$ showed that ICA decreased the higher $A\beta_{1-40}$ burden in APP/PS1 mice [$F_{(3,12)} = 9.404$, $P = 0.002$]. (F) Quantitative analysis of $A\beta_{1-42}$, ICA also decreased $A\beta_{1-42}$ burden [$F_{(3,12)} = 18.971$, $P < 0.001$]. Data were expressed as mean ± S.E.M, $^{**}P < 0.01$ vs. WT + ddH_2O, $^{\#}P < 0.05$, $^{\#\#}P < 0.01$ vs. APP/PS1 + ddH_2O ($n = 4$).

Epimedium is a traditional Chinese herbal medicine used to enhance sexual function, strengthen bones and muscles, and treat diseases for nearly a thousand years. Icariin (ICA, $C_{33}H_{40}O_{15}$, molecular weight 676.67), an active compound of epimedium [7], has a wide range of pharmacological effects, such as anti-osteoporotic, anti-inflammatory, and antidepressant activities [8,9]. Previous studies including our work showed that ICA has the function of protecting neurons and preventing AD models [10–19], however, the effect of ICA on ER stress under AD condition still need to explore. Therefore, this study aimed to investigate whether ICA suppress ER stress in AD model and further exploring the underlying mechanisms.

2. Materials and methods

2.1. Ethic statement

All animal experiments were performed in accordance with Chinese Guidelines of Animal Care and Welfare, and the present study was approved by the Animal Care and Use Committee of Zunyi Medical University (Zunyi, China).

2.2. Materials

ICA (purity ≥ 98% by HPLC) was purchased from Nanjing Zelang Medical Technology Co., Ltd. (Nanjing, China), and it was dissolved in double-distilled water and mixed by ultrasonic for 8 min. All reagents were reagent-graded and commercially available.

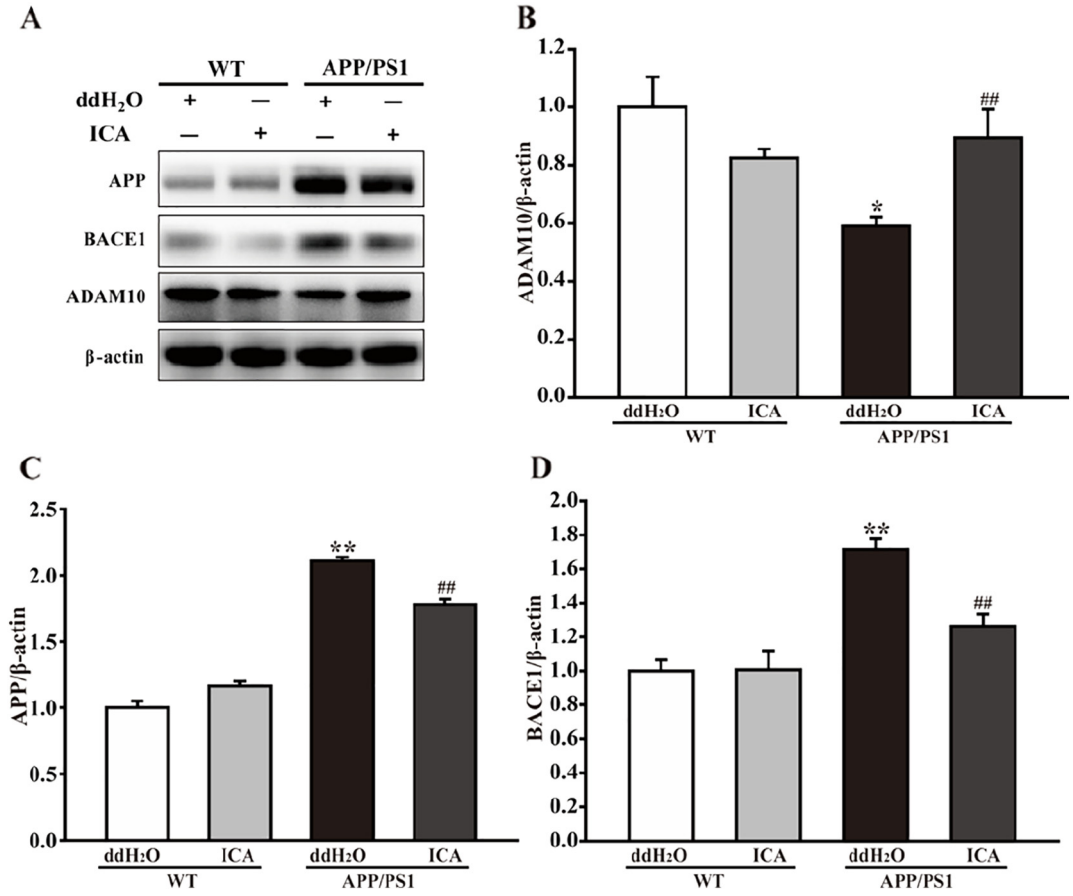

Fig. 4. Effects of ICA on APP process in the hippocampus of APP/PS1 mice. (A) The bands of APP, BACE1, ADAM10 were tested by Western blot. (B–D) Quantitative analysis of the bands, there were significant decreased expression followed ICA treatment of APP [$F_{(3,12)} = 73.337$, $P < 0.001$], BACE1 [$F_{(3,12)} = 11.611$, $P = 0.001$], and ADAM10 [$F_{(3,12)} = 7.955$, $P = 0.003$]. Data were expressed as mean ± S.E.M, $^{*}P < 0.05$, $^{**}P < 0.01$ vs. WT + ddH_2O, $^{\#\#}P < 0.01$vs. APP/PS1 + ddH_2O ($n = 4$).

2.3. Animals

Nine months old male APP/PS1 transgenic mice and age, gender-matched wild type (WT) mice (weight 35 to 45 g) were purchased from Nanjing University-Nanjing Institute of Biomedical Sciences, License Number: SCXK (JiangSun, China) 2015-001. Experimental mice were raised in the SPF animal room, kept in a quiet, 12-hour day/night cycle, relatively constant room temperature (23 ± 1 °C) and humidity (60 ± 2%), and animals were free to drink and food.

2.4. Animal treatments

These mice were randomly divided into: WT control and WT + ICA, as well APP/PS1 control and APP/PS1 + ICA groups, respectively. Treated mice were orally administered with ICA at a dose of 60 mg/kg body weight daily, and control mice received volume-matched stilled water for 3 months.

2.5. Morris water maze test

The Morris water maze (MWM) assay consisted of 4 days of the spatial learning and memory training, and a probe trial applied on day 5. The MWM consisted of a large circular black pool (120 cm in diameter and 50 cm in height) filled with water (23 ± 2 °C and 30 cm in depth), which was divided into four quadrants. In the pool, a hidden of 12 cm diameter was located 1 cm below the water level in the center of the target quadrant throughout the 4-day training period. The four consecutive days, mice were trained in every morning and afternoon. And the escape latency of mice to reach the hidden platform was recorded. Mouse was given 60 s to search the platform and kept on the platform for 20 s, if a mouse did not find the platform within 60 s, its escape latency was recorded as 60 s, while it was gently guided to the platform and stayed on there for 20 s. On the fifth day, a probe test was formed by removing the platform and allowing each mouse to swim freely for 60 s in the pool. During the test, the time spent in the target quadrant and the frequency crossing the target quadrant was measured by the TopScan Topview Behavior Analyzing System (TopScan Version 3.00).

2.6. Object recognition test

The object recognition test (ORT) detects the learning and memory ability of mice, and the device is mainly composed of reaction box (40 cm × 40 cm × 40 cm), automatic recording analysis System. The objects chosen were 2 identical cuboid green plastic blocks (A, 5 cm × 5 cm × 5 cm), and a white cylindrical block (B, height: 5 cm; diameter: 4 cm). The two reaction chambers were placed in a quiet room, and two identical objects were placed in the same corners of the two reaction chambers two days ago, and a mouse was free to move in the reaction chamber. On the 3rd day, one object (A) was changed to a B object, and the mouse was free to move and observe for 10 min. The time spend on object A means familiar (F), and time on object B is recorded as new (N). The memory discrimination index (DI) = (N − F) / (N + F), the level of DI was considered as a reflection of memory ability in this study.

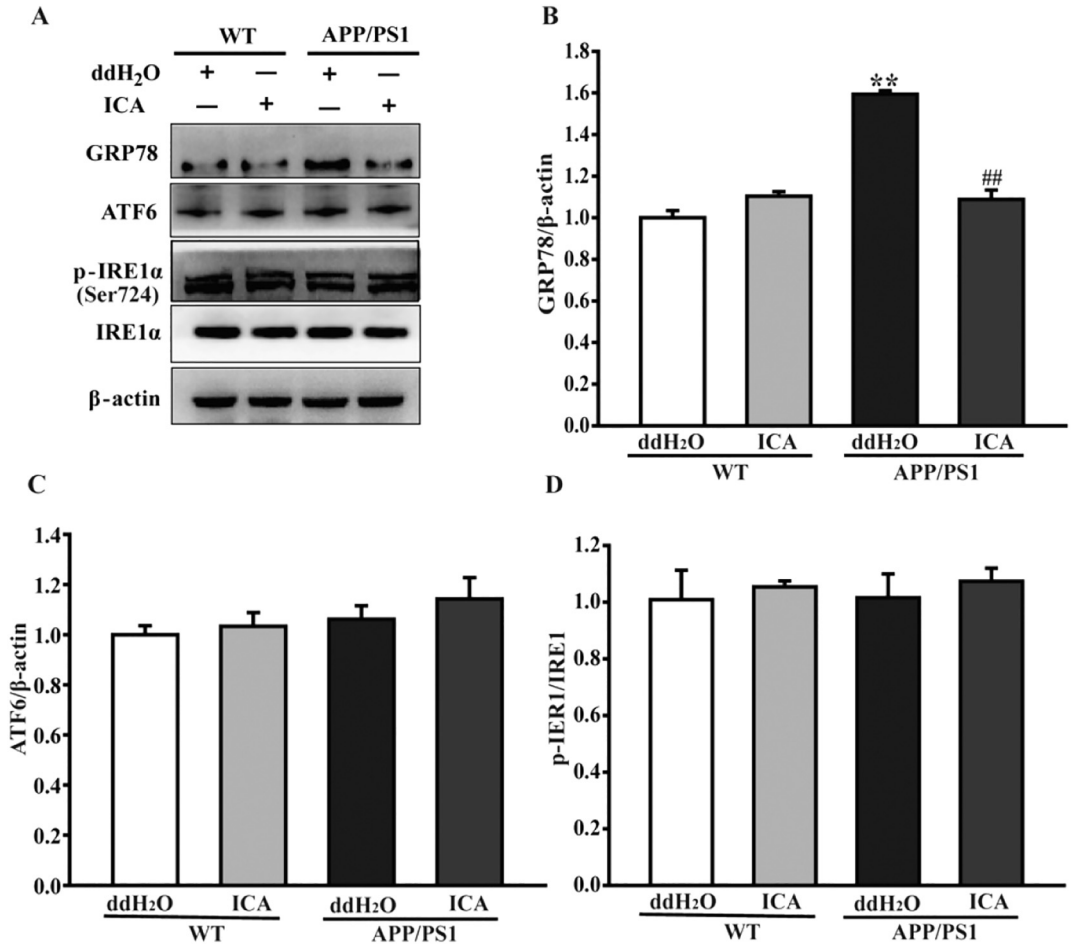

Fig. 5. Effects of ICA on ER stress in the hippocampus of APP/PS1 mice. ER stress was activated in the hippocampus of APP/PS1 mice evidenced by the high levels of GRP78, ATF6, and p-IRE1α. ICA treatment decreased GRP78 level, not affected the ATF6, IRE1α and IRE1α phosphorylation. (A) Immunoblots. (B–D) Quantitative analysis of the above proteins in every groups: GRP78 [$F_{(3,12)} = 51.074$, $P < 0.001$], ATF6 [$F_{(3,12)} = 0.918$, $P = 0.462$]. p-IRE1α/IRE1α ratio [$F_{(3,12)} = 0.329$, $P = 0.804$]. Data were expressed as mean ± S.E.M, $^{**}P < 0.01$ vs. WT + ddH_2O, $^{\#\#}P < 0.01$vs. APP/PS1 + ddH_2O ($n = 4$).

2.7. Nissl staining

After the behavioral experiments, four mice of each group were given anesthesia with pentobarbital sodium (50 mg/kg), and then these mice were perfused via the ascending aorta in 0.1 M phosphate-buffered saline (PBS), and 4% polyformaldehyde. The brains were removed and post-fixed with the same fix solution for one week and were cut into coronal sections for Nissl staining. The histopathological abnormalities were examined under a light microscope.

2.8. Immunofluorescence

For the immunofluorescence staining, 5 μm brain slides were taken through the hippocampus in free-floating conditions, and were dried at 60 °C for 30 min. The following steps were that: (1) washed with PBS and incubated in PBS with 0.3% Triton-X 100 for 30 min, (2) blocked in 20% goat serum (GIBCO Invitrogen) for 1 h, (3) incubated with primary antibody Aβ (AB5076, 1:200, Merck-millipore, USA) at 4 °C overnight, (4) washed and incubated for 1 h at room temperature with fluorescent Alexa-594 secondary antibody (A21203, 1:500, Thermo Fisher Scientific, USA), (5) photographed under fluorescence microscope (Olympus BX53, Olympus, Japan).

2.9. TUNEL staining

Paraffin sections were routinely dewaxed, washed twice with double distilled water, 5 min each, 3% H_2O_2 extinguished endogenous enzymes, incubated at 37 °C for 17 min in the dark, washed three times with PBS for 15 min. The sections were treated with 20 μg/mL Proteinase K working solution, digested in a wet box at 37 °C for 13 min, and washed PBS 3 times for 5 min each time. TUNEL reaction mixture (Enzyme Solution:Lable Solution = 1:50) was added to each section, 37 °C in a dark box for 1 h, PBS rinsed 3 times, each time for 10 min. DAPI stained cell nucleus for 5 min and xylene gradient transparent, neutral gum seal.

2.10. Real-time RT-PCR

Total RNA was isolated from hippocampus using Trizol (TakaRa Biotechnology, Dalian, China) reagent following the manufacturer's instructions. The quality and quantity of RNA were determined by the Nano Drop (Thermo Scientific, ND-2000, USA), with 1.8 < 260/280 ratio < 2.1. Total RNA was reversely transcribed with a High Capacity Reverse Transcriptase Kit (Applied Biosystems, Foster City, CA, USA). The primers were designed with Primer3 software and listed (Table 1). The 15 μL PCR reaction mix contained 3 μl of cDNA (10 ng/μl), 7.5 μl of iQ™ SYBR Green Supermix (Bio-Rad Laboratories, Hercules, CA), 0.5 μl of primers mix (10 μM each), and 4 μl of non-RNase H_2O. After 5 min denature at 95 °C, 40 cycles will be performed: annealing and extension at 60 °C for 45 s and denature at 95 °C for 10 s. Dissociation curve was performed after finishing 40 cycles to verify the quality of primers and amplification. Relative expression of genes was calculated by the

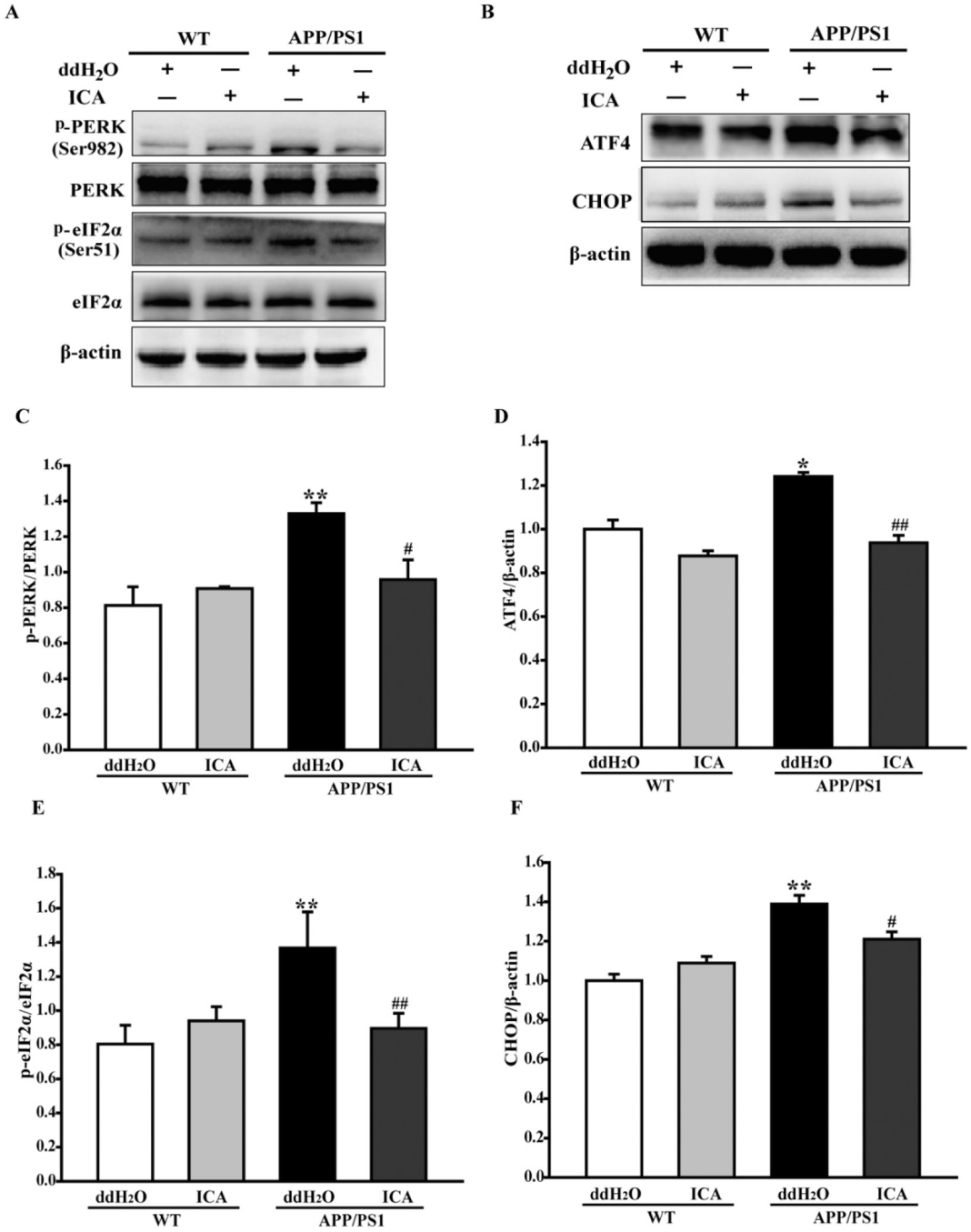

Fig. 6. Effects of ICA on the PERK signaling in the hippocampus of APP/PS1 mice. The phosphorylation of PERK and eIF2α, as well ATF4 and CHOP proteins expression were increased in APP/PS1 mice, ICA treatment significantly decreased their levels. (A, B) Immunoblots of PERK, p-PERK, eIF2α, p-eIF2α, ATF4 and CHOP. (C–E) Quantitative analysis of abovementioned proteins: p-PERK/PERK ratio [$F_{(3,12)} = 7.564$, $P = 0.004$], p-eIF2α/eIF2α ratio [$F_{(3,12)} = 14.036$, $P < 0.001$], ATF4 [$F_{(3,12)} = 25.892$, $P < 0.001$] and CHOP protein [$F_{(3,12)} = 18.594$, $P < 0.001$]. The relative OD was normalized to β-actin. Data were expressed as mean ± S.E.M, $^{*}P < 0.05$, $^{**}P < 0.01$ vs. WT + ddH_2O, $^{\#}P < 0.05$, $^{\#\#}P < 0.01$vs. APP/PS1 + ddH_2O ($n = 4$).

$2^{-\Delta\Delta Ct}$ method and normalized to β-actin and expressed as % of control. The following TaqMan probes from the universal probe library were used:

2.11. Western blot

Western blot analysis was used to determine the level of APP (ab32136), $A\beta_{1-42}$ (ab201061), BACE1 (D220305, BBI, China), $A\beta_{1-40}$ (MAB2675, abnova, China), ADAM10 (25900-1-AP), GRP78 (D151791, Sangon Biotech, China), ATF6 (24169-1-AP), PERK (20582-1-AP), eIF2α (11233-1-AP), ATF4 (20582-1-AP), CHOP (15204-1-AP), caspase-3 (19677-1-AP), caspase-9 (10380-1-AP), GAPDH (10494-1-AP) (from Proteintech, China), IRE1 (DF7709), phospho-IRE1 (Thr724, DF8322), phospho-PERK (Thr982, DF7576), phospho-eIF2α (AF3087), Bcl-2 (AF6139), Bax (AF0120), β-actin (AF7018) (from Affinity, USA), caspase-12 (2202S, CST, USA). Hippocampi (n = 4 each group) were homogenized in the radio-immunoprecipitation assay (RIPA) lysis buffer containing protease inhibitors and phosphatase inhibitors (100 μM) on an ice box. The homogenates were centrifuged for 10 min (12,000 rpm, 4 °C), and supernatants were extracted and stored at −80 °C. Protein concentration was tested by BCA protein assay kit (Beyotime, China). The samples (25–30 μg) were heat-denatured at

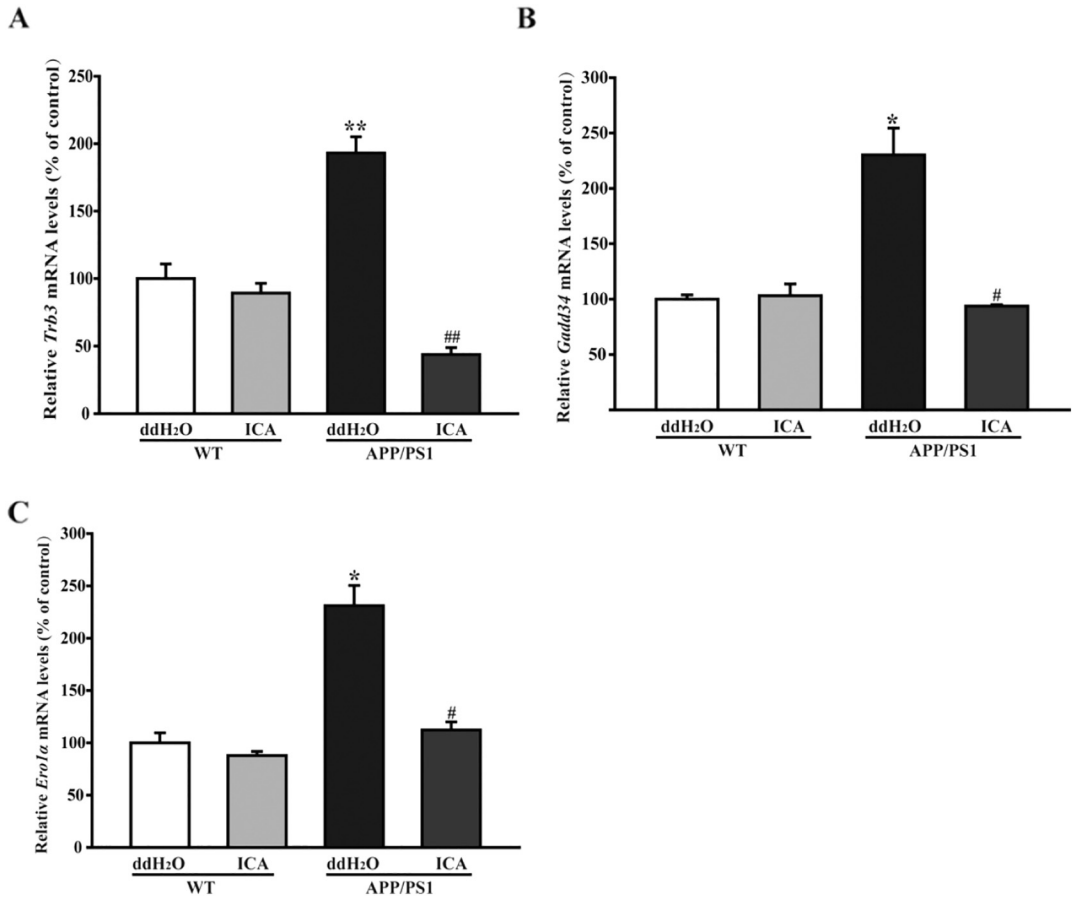

Fig. 7. Effects of ICA on ER stress in the hippocampus of APP/PS1 mice. The phosphorylation of TRB3 mRNA, GADD34 mRNA and ERO1α mRNA expression were increased in APP/PS1 mice, ICA treatment significantly decreased their expression. The mRNA expression of (A) TRB3 [$F_{(3,12)} = 46.234$, $P < 0.00$], (B) GADD34 [$F_{(3,12)} = 23.559$, $P < 0.001$], (C) ERO1α [$F_{(3,12)} = 32.427$, $P < 0.001$] was measured by quantitative real-time PCR, normalized to β-actin. Data were expressed as mean ± S.E.M, $^{*}P < 0.05$, $^{**}P < 0.01$ vs WT + ddH_2O, $^{\#}P < 0.05$, $^{\#\#}P < 0.01$vs. APP/PS1 + ddH_2O (n = 4).

95 °C for 10 min and separated by 5% SDS-PAGE gel at 60 V as well as the 8–10% SDS-PAGE gels at 120 V, then transferred onto Polyvinylidene difluoride (PVDF) membranes (0.45 μm) at 25 V for 30–40 min. Membranes were blocked with 5% non-fat milk in 0.05% TBST for 2 h at room temperature and incubated with these above-mentioned primary antibodies at 4 °C over night. After washing, the membranes were incubated with appropriate HRP-conjugated secondary antibodies (Beyotime, China) for an hour at room temperature. Then ECL Reagent (Millipore Corporation, USA) and Image Lab (Bio-Rad) were used to analyze the protein bands.

2.12. Statistical analysis

Statistical analysis was performed by SPSS software (Chicago, IL, USA). Data were expressed as mean ± S.E.M, the escape latency of Morris water maze assay was analyzed with repeated measures analysis of variance ANOVA, followed by Bonferroni multiple comparison test; the crossing platform number was analyzed by Kruskal-Wallis H test; the changes Aβ burden stained by immunofluorescence between APP/PS1 mice and treated with ICA were analyzed by independent samples *t*-test; the others were analyzed using a one-way ANOVA followed by Bonferroni multiple comparisons test. Significant *p*-value was considered < 0.05.

3. Results

3.1. Effect of ICA on learning and memory function of APP/PS1 transgenic mice

Marris water maze was used to evaluate the effects of ICA on APP/PS1 mice learning and memory capacity (Fig. 1). The escape latency data of navigation experiment was gradually shortened with daily training, ICA mice showed a significant reversion of the impaired memory capacity observed in APP/PS1 mice with decreased escape latency on the fourth day of training ($P < 0.01$, Fig. 1A). The spatial probe test was performed on the 5th day, the time spent in the target quadrant and the frequency crossing target quadrant was recorded, significant difference was found in ICA treated mice compared with APP/PS1 mice ($P < 0.05$, Fig. 1B, C).

In the object recognition test, there were no significant alternations among groups on the first 2 days (data not shown). On day 3, the time contacting new and old objects of mice was shown in Fig. 2A, and APP/PS1 mice were decreased in the memory discrimination index (DI) compared with WT group, however, DI was increased significantly after ICA treatment ($P < 0.05$). Taken together, behavior results indicated that ICA treatment could ameliorate learning and memory impairments of APP/PS1 mice ($P < 0.05$, Fig. 2B).

3.2. Effects of ICA on APP-Aβ process in the hippocampus of APP/PS1 mice

$Aβ_{1–42}$ and $Aβ_{1–40}$ are more neurotoxic and likely to aggregate to form plaque [20]. Immunofluorescence staining (Fig. 3A) with antibody

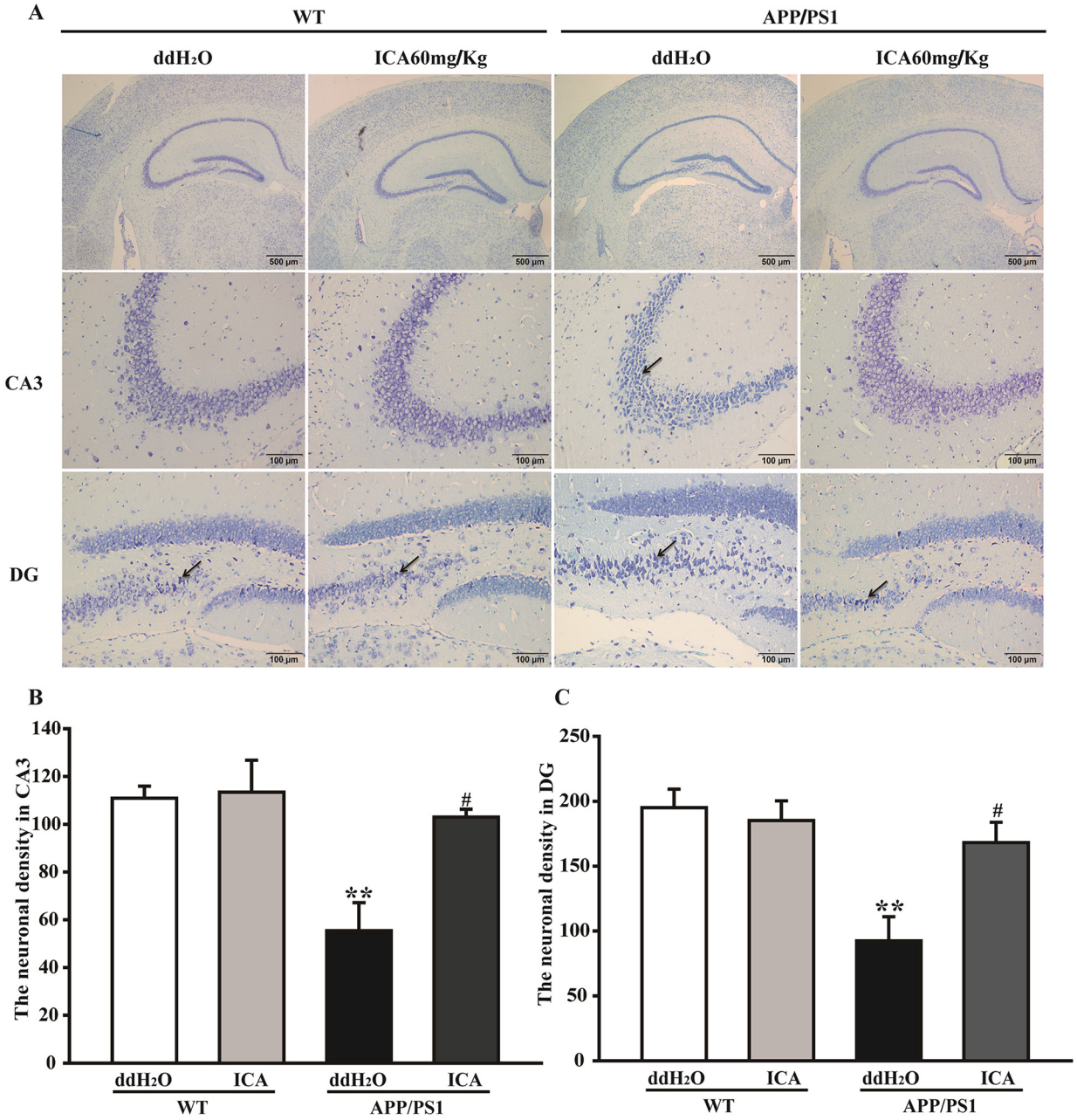

Fig. 8. Effect of ICA on neurons loss in the hippocampus of APP/PS1 mice. Significant decrease in the number of surviving neurons in hippocampal CA3 and DG regions of APP/PS1 transgenic mice, and long-term administration of ICA can maintain the number of surviving neurons in hippocampus. (A) Representative photomicrographs of Nissl staining results of each group were shown in Fig. 3A (magnification 200×, scale bar = 100 μm). (B, C) Statistics of viable neurons in the hippocampal CA3 and DG regions [$F_{(3,12)} = 8.415$, $P = 0.003$, $F_{(3,12)} = 8.199$, $P = 0.003$]. Note: values were expressed as mean ± S.E.M, $^{*}P < 0.05$, $^{**}P < 0.01$ vs. WT + ddH_2O, $^{\#}P < 0.05$ vs. APP/PS1 + ddH_2O ($n = 4$).

against Aβ was used to test the total Aβ burden in mouse brain. Aβ deposition was significantly increased in the hippocampal DG region of APP/PS1 group compared with the WT group ($P < 0.01$). APP/PS1 mice treated with ICA showed an obvious decrease in Aβ deposition ($P < 0.05$, Fig. 3B). Meanwhile, we further examined $Aβ_{1–42}$ and $Aβ_{1–40}$ load via western blot, the results were in line with Aβ staining, the levels of $Aβ_{1–42}$ and $Aβ_{1–40}$ were significantly increased in the hippocampus of APP/PS1 ($P < 0.01$). Both $Aβ_{1–42}$ and $Aβ_{1–40}$ levels were decreased following treatment with ICA ($Aβ_{1–42}$: $P < 0.05$, $Aβ_{1–40}$: $P < 0.01$, Fig. 3C, D). We further observed the level of Aβ precursor, APP, and its process (Fig. 4A–D). These results showed that APP protein expression was significantly increased in APP/PS1 group ($P < 0.01$), while ICA treatment markedly down regulated it ($P < 0.01$, Fig. 4C). Moreover, ADAM10 protein was dramatically reduced in APP/PS1 mice ($P < 0.05$). In contrast, BACE1 protein was significantly enhanced ($P < 0.01$). Interestingly, ICA could blunt the down regulation of ADAM10 ($P < 0.01$, Fig. 4B), also down-regulated BACE1 protein ($P < 0.01$, Fig. 4D). These results may suggest that ICA inhibited Aβ production via reducing APP amyloidogenesis process, which is in line with previous studies [21].

3.3. Effects of ICA on ER stress in the hippocampus of APP/PS1 mice

Excessive aggregation of APP and Aβ in ER and intracellular calcium imbalance can lead to endoplasmic reticulum stress. Thus, we examined the ER stress marker GRP78 protein level, and main stress

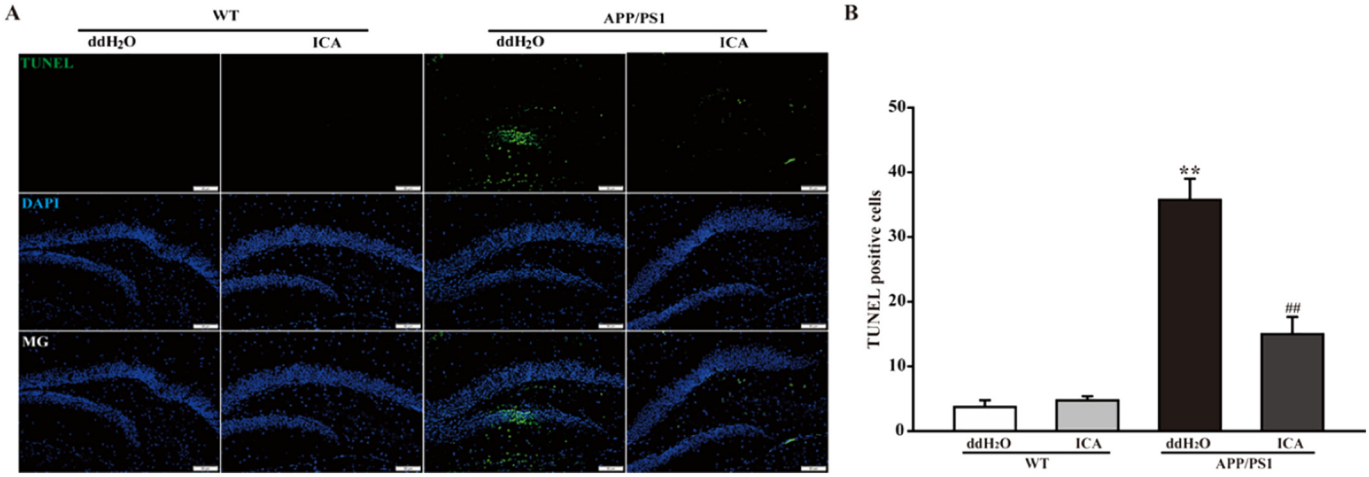

Fig. 9. Effects of ICA on apoptosis in the APP/PS1 mice. A large number of TUNEL stained green nuclei appeared in the hippocampus of APP/PS1 transgenic mice in DG region, and the number of neuronal apoptosis increased. Long-term administration of ICA could reduce neuronal apoptosis. (A) TUNEL staining of hippocampus DG region sections (magnification 200×, scale bar 50 μm). (B) Quantitative analysis of apoptotic cells in the hippocampus DG region [$F_{(3,12)} = 46.409$, $P < 0.001$]. Data were expressed as mean ± S.E.M, $^{**}P < 0.01$ vs. WT + ddH_2O, $^{\#\#}P < 0.01$vs. APP/PS1 + ddH_2O (n = 4). (For interpretation of the references to color in this figure legend, the reader is referred to the web version of this article.)

sensors protein expression and phosphorylation level of IRE1α, PERK, eIF2α, and ATF6. A number of results showed that GRP78 was increased in APP/PS1 ($P < 0.01$), ICA treatment markedly reduced GRP78 level ($P < 0.01$, Fig. 5A, B), no significant changes of IRE1α and ATF6 were found ($P > 0.05$, $P > 0.05$, Fig. 5C, D), however, the PERK/eIF2α pathway may be involved in the effect of ICA on ER stress, evidenced by ICA inhibiting the phosphorylation of PERK and its downstream eIF2α phosphorylation level ($P < 0.05$, $P < 0.05$, Fig. 6A, C, E). We further examined the downstream factors of eIF2α: ATF4 and CHOP protein, and found that both ATF4 and CHOP in APP/PS1 mice were much higher than WT mice ($P < 0.01$, $P < 0.01$), ICA significantly down-regulated both two proteins expression (ATF4: $P < 0.01$, CHOP: $P < 0.05$, Fig. 6B, D, F).

Then, we examined the target genes of ATF4 and CHOP: TRB3, GADD34, and ERO1α (Fig. 7). The results showed that the mRNA levels of TRB3, GADD34, and ERO1α in APP/PS1 mice were significantly higher than WT group ($P < 0.01$, $P < 0.05$, $P < 0.05$). After ICA treatment, the mRNA levels of TRB3, GADD34, and ERO1α were significantly inhibited ($P < 0.01$, $P < 0.05$, $P < 0.05$, Fig. 7A, B, C). These indicated that ICA may inhibit ER stress in APP/PS1 mice via suppressing the PERK/eIF2α signaling pathway.

3.4. Effects of ICA on apoptosis in the APP/PS1 mice

Activated PERK pathway induces apoptotic cell production [22], CHOP is an important signaling molecule from survival to apoptosis [23]. To investigate the effect of ICA on neuron, we used Nissl staining (Fig. 8A) and TUNEL (Fig. 9) assay to observe the morphological changes of neurons and apoptosis followed ICA treatment. Most hippocampal neurons were pyknotic and atrophied with irregular shape, a tangled appearance and apoptosis cells in the hippocampus of APP/PS1 mice, after ICA treatment the neuronal density was increased in CA3 and DG regions ($P < 0.05$, Fig. 8B, C).

Then, we tested the neuronal apoptosis and close relative proteins, the results showed that a large number of TUNEL-stained green nuclei were found in the hippocampal DG region of APP/PS1 mice (Fig. 9), the Bax/Bcl-2 ratio was higher, as well cleaved caspase-12, -9 and -3 levels were increased in APP/PS1 mice compared to WT mice. However, ICA treatment partly reversed the abovementioned parameters, including that the number of TUNEL positive cells (Fig. 9), cleaved caspase-12, -9 and -3 levels (Fig. 10) decreased; the Bax/Bcl-2 ratio (Fig. 10) increased followed ICA treatment. The above findings indicated that apoptosis reduced in ICA treatment mice was partly relative to suppressing ER stress.

4. Discussion

Our pre-tested the effect of ICA on ER stress in vitro induced by H_2O_2 and tunicamycin, considering the protection of ICA on central nervous system reviewed in Angeloni [19], here, we have chosen APP/PS1 transgenic mice in this study mimicking AD pathological features to investigate the role of ICA anti-ER stress, and found that the performance of APP/PS1 mice in behavior tests was exacerbated, in line with the previous reports [24–26], ICA treated mice showed a significant reversion of the memory impairment observed on this AD model, with suppressing the APP-Aβ pathway and ER stress in the hippocampus of AD mice.

Senile plaques formed by extracellular Aβ deposition are widely recognized as a key pathological feature of AD and represent the most important neuropathological histological features of AD [27]. Increasingly evidence showed that Aβ deposition in APP/PS1 transgenic mouse beginning form 9 months age and gradually increasing with age [28]. We used immunofluorescence staining against Aβ antibody to observe the effect of ICA and found that ICA effectively decreased the Aβ deposition in APP/PS1 mouse brain. Aβ precursor (APP) and β-secretase (BACE1) have been reported highly expression in AD patients' brains [29], furthermore, their abnormal levels promote the production of Aβ in AD mice [20]. So, we observed the APP protein level and process following ICA under AD condition, the results consisted with previous reports that ICA decreased the APP level, which may be related to inhibit APP amyloidgenesis pathway by decreasing the expression of BACE1. ADAM10 has been considered as a neuroprotective and neurotrophic effect and defined as the most important member of the ADAMs family of alpha-secretases, which is critical for neurogenesis and embryonic brain development [30]. Interestingly treatment with ICA significantly induced ADAM10 expression in the hippocampus of APP/PS1 mice. Our results clearly confirmed that ICA ameliorates the memory function of APP/PS1 mice, as well suppresses the APP-Aβ pathway.

As an important organelle in eukaryotic cell, ER is closely related to the synthesis of proteins, the production of lipids and the storage of calcium ions [31]. It has been reported that a variety of causes, such as ischemia, low oxygen, drug or poison, oxidative stress and other pathological physiology stimuli could induce ER stress further to induce

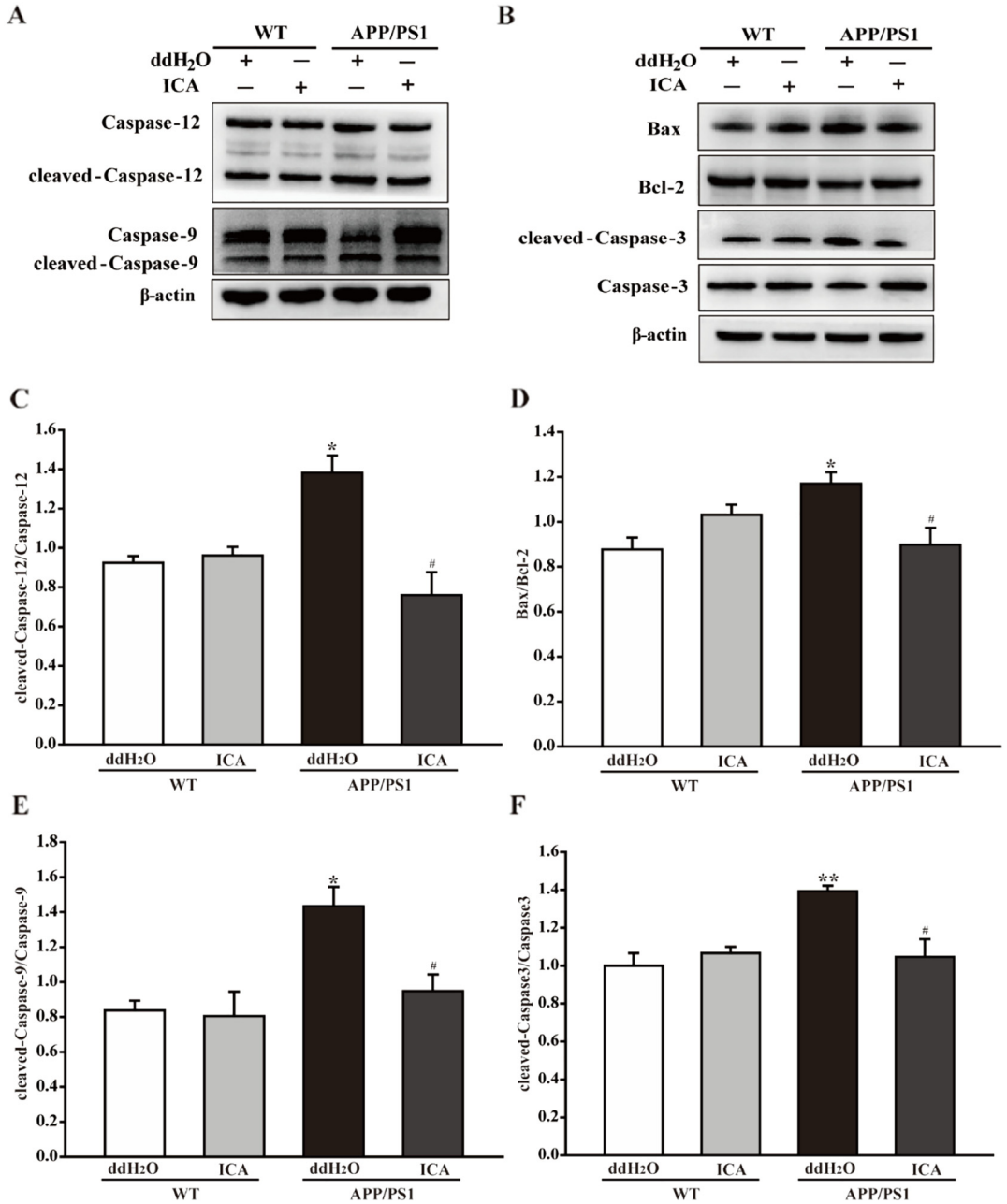

Fig. 10. Effects of ICA on apoptosis in the APP/PS1 mice. The intracellular apoptosis cascade reaction of hippocampal Caspases family was activated, and the ratio of Bax/Bcl-2/ was significantly increased in APP/PS1 transgenic mice. After long-term treatment, ICA significantly inhibited the activation of Caspase-12, Caspase-9 and Caspase-3, including Caspase family, in the hippocampus of APP/PS1 transgenic mice, down-regulated the ratio of Bax/Bcl-2 and inhibited neuronal apoptosis. (A) The antibody-reactive band of the cleaved-Caspase-12, cleaved-Caspase-9 and Caspase-12, Caspase-9. (B) The antibody-reactive band of the Bax/Bcl-2, cleaved-Caspase-3 and Caspase-3, respectively. (C) cleaved-Caspase-12/Caspase-12 ratio [$F_{(3,12)} = 11.598$, $P = 0.001$]. The relative OD was normalized to β-actin. (D) Bax/Bcl-2 ratio [$F_{(3,12)} = 5.556$, $P = 0.013$]. The relative OD was normalized to β-actin. (E) Cleaved-Caspase-9/Caspase-9 ratio [$F_{(3,12)} = 7.638$, $P = 0.004$]. The relative OD was normalized to β-actin. (F) Cleaved-Caspase-3/Caspase-3 ratio [$F_{(3,12)} = 12.550$, $P = 0.001$]. The relative OD was normalized to β-actin. Data were expressed as mean ± S.E.M, $^{*}P < 0.05$, $^{**}P < 0.01$ vs. WT + ddH_2O, $^{\#}P < 0.05$vs. APP/PS1 + ddH_2O (n = 4).

the cell self-adjustment and even apoptosis [32]. And also, ER stress is ubiquitous in AD brain; the apoptosis induced by ER stress is reported as a possible cause of neurodegenerative diseases []. There are three main sensors, PERK, ATF6 and IRE1 located in ER membrane, normally combined with GRP78 which closes their signals. Conversantly, under chronic or irreversible ER stress, GRP78 dissociates from the sensors and binds to non-folded and folded proteins, which is an important marker to induce and reflect the stress level of ER, and then the sensor proteins will be activated and trigger cell apoptosis through multiple pathway [33]. In this study, we found that there was ER stress occurred in APP/PS1 mice hippocampus with ER stress markers high level, however, the ER stress was suppressed by ICA treatment with decreasing the GRP78 protein level.

Our results showed that had high of in hippocampus, and the treatment with ICA significantly reduced the expression of GRP78 in the hippocampus. When cellular ERS, dissociation of GRP78, ATF6 is transported to Golgi, and is cleaved by protease site 1 protease and site 2 protease, the release of ATF6 fragment into the nucleus, activating UPR target gene expression, but also activate gene transcription of X-box binding protein-1 (XBP1) [34]. Furthermore, IRE1 is a type I

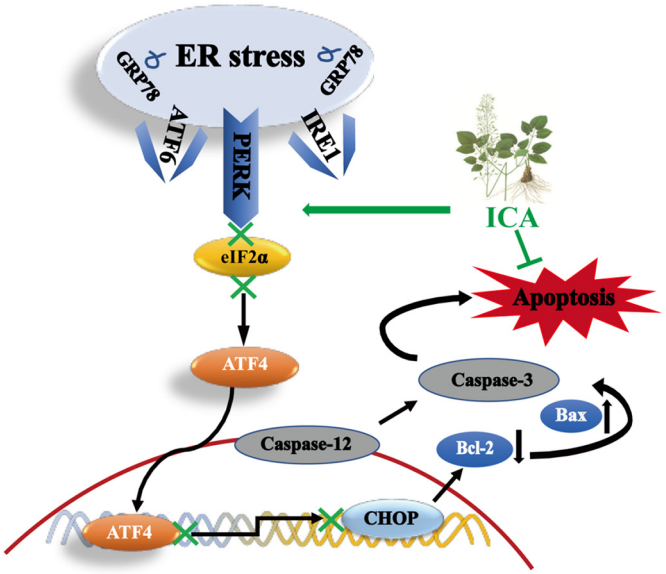

Fig. 11. Overview diagram illustrates the mechanism of ICA inhibits ER stress-mediated neuronal apoptosis. When ER stress occurs, with a large number of GRP78 unfolded protein binding, and the PERK, IRE1, ATF6 separated, and the ICA can be suppressed to suppress the expression of GRP78 and PERK/eIF2α signaling pathway, and to further suppress the expression of Bcl-2 protein, thereby reducing hippocampal neurons apoptosis.

protein on the ER membrane and has two subtypes of IRE1α and IRE1β in mammals. IRE1α expressed in all cells, the ER lumen sensed when unfolded protein aggregation, IRE1α be activated by oligomerization and autophosphorylation. IRE1 has protein kinase and endonuclease dienzyme activity. Activated IRE1 cleaves XBP1 mRNA, which encodes the transcriptional activator XBP1 splicing to promote cell survival, while un-cleaved XBP1 mRNA encodes the transcriptional repressor XBP1 un-splicing; and the further recruitment of activated IRE1 tumor necrosis factor receptor-associated factor-2, activation of downstream signal Jun N-terminal kinase pathway and leads to activation of caspase-12 cell apoptosis; In addition, the IRE1 positioning of cutting mRNA degradation, thereby reducing ER burden [35]. Interestingly, we did not observe a significant change in ATF6 protein expression and phosphorylated IRE1α at Ser724 in hippocampus of APP/PS1 transgenic mice. PERK is also an important signaling pathway for endoplasmic reticulum stress. When PERK phosphorylates the downstream substrate eIF2α, phosphorylation of eIF2α inhibits protein synthesis, thereby reducing the ER burden, while increasing the transcription factor translation ATF4 and activating transcription factor expression ATF4 downstream protein CHOP further induce UPR target gene GADD34, TRB3 and ERO1α etc., while inhibiting Bcl-2 expression leads to apoptosis [22]. Our results indicate that ICA after long-term treatment reduces the phosphorylation levels of PERK at Ser982 and eIF2α at Ser51, and decreases the protein expression of ATF4 and CHOP, which can effectively inhibit the activation of PERK signaling pathway. The PERK pathway is found to be active in brain tissue of AD patients, whereas premature protein mutations can be increased by eIF2α phosphorylation in the PERK pathway to reduce protein accumulation [36]. Moreover, we found high expression of ATF4 and highly phosphorylated eIF2α and PERK in the brain of AD patients, and phosphorylated eIF2α and PERK were mainly concentrated in hippocampal neurons [29]. ERS induced apoptosis play a crucial role in many diseases such as diabetes, neurodegenerative diseases, and especially AD []. Given the fact that hippocampus neuronal apoptosis is one of the major causes of memory loss accompanied by neurodegeneration [37], cell apoptosis was further investigated. TUNEL assay showed a significant number of TUNEL positive cells in the hippocampus of APP/PS1 transgenic mice. In agreement with the effect of neuroprotection, ICA treatment significantly decreased the apoptotic cells in APP/PS1 transgenic mice. Aβ can cause ERS and its mediated apoptosis. The mouse neurons treated with Aβ have increased Caspase-12 activation, which increased the activation of Caspase-12, increased of LDH release, and decreased hippocampal activity in the brain of AD patients [38].

Moreover, intracellular apoptotic cascade including caspases family can be triggered, and activation of Caspase-12 stimulates the caspase cascade and ultimately activates Caspase-9 and Caspase-3, which leads to the increases in apoptotic responses under Aβ toxicity [39,40]. The results of this experiment show that the levels of Caspase-12, Caspase-9 and Caspase-3 are decreased in the brain of APP/PS1 transgenic mice and the activation of Caspase-12, Caspase-9 and Caspase-3 were increased in the hippocampus. However, ICA significantly inhibited the activation of Caspase-12, Caspase-9, and Caspase-3 in the hippocampus of APP/PS1 transgenic mice. Taken together, these data suggest that ICA may serve as an effective anti-apoptotic agent that inhibits Aβ deposition-induced apoptosis in APP/PS1 transgenic mice. Various molecules including the caspase family have been found to be involved in the mechanism of apoptosis, and Bcl-2 family members are the most studied molecules regulating apoptosis [41]. Bcl-2 is an anti-apoptotic member of the Bcl-2 family and Bax is a pro-apoptotic member that acts in a manner opposite to Bcl-2. The ratio of Bax/Bcl-2 has been a key factor in determine cell survival and death. Down-regulation of Bcl-2 and up-regulation of Bax in APP/PS1 were found transgenic mice. Our results are consistent with previous studies suggesting that Bcl-2 family proteins regulate apoptosis after Aβ deposition induced ERS, and further demonstrate that ICA treatment attenuates hippocampal neuronal cell death by decreasing the ratio of Bax/Bcl-2. Taken together, these data suggest that ICA may serve as an effective anti-apoptotic agent that inhibits endoplasmic reticulum stress induced by Aβ deposition in APP/PS1 transgenic mice and produces anti-apoptotic effects.

In summary (Fig. 11), this study demonstrates that ICA as a broad-spectrum anti-cancer natural compound that can significantly impair learning and memory impairment interferes with multiple pathogenic mechanisms, including decreasing Aβ deposition and degradation in APP/PS1 in transgenic mice. The protective mechanism may be due to increased activation of ADAM10 and inhibition of APP and BACE1 expression, which appear to be due to inhibition of the PERK/eIF2α signaling pathway, which reduces apoptosis induced by ERS. Taken together, the findings provide strong evidence that ICA may be developed as a potently promising natural compound candidate for halting progression of AD.

5. Conclusion

In conclusion, the present study demonstrates that ICA could attenuate spatial learning and memory impairments in APP/PS1 transgenic mice. These results suggest that ICA could decrease the ER stress and apoptosis in APP/PS1 transgenic mice, may be through inhibiting the PERK/eIF2α pathway. Therefore, suggesting that ICA might be a promising potential compound for the treatment of AD. Since AD is the main health burden in the world, the incidence is getting higher and higher, and affects the quality of life of people, the present study is of immense significance.

Declaration of competing interest

None declared.

Acknowledgments

This work was supported by the National Natural Science Foundation of China (Grant No. 81560594), International Science and Technology Cooperation Program of Guizhou Province (Qiankehe G [2014]7011), Shijingshan's Tutor Studio of Pharmacology [GZS-

2016(07)].

References

[1] B. Paola, P. Christina, The state of the art of dementia research: new frontiers. Every 3 seconds! The scale of the challenge, C. World Alzheimer Report 2018, Alzheimer's Disease International, London, 2018, pp. 1–48.

[2] Y. Cai, J. Arikkath, L. Yang, Interplay of endoplasmic reticulum stress and autophagy in neurodegenerative disorders, Autophagy 12 (2016) 225–244.

[3] H. Kadowaki, H. Nishitoh, Signaling pathways from the endoplasmic reticulum and their roles in disease, Genes 4 (2013) 306–333.

[4] M. Obulesu, M.J. Lakshmi, Apoptosis in Alzheimer's disease: an understanding of the physiology, pathology and therapeutic avenues, Neurochem. Res. 39 (2014) 2301–2312.

[5] W. Paschen, Endoplasmic reticulum: a primary target in various acute disorders and degenerative diseases of the brain, Cell Calcium 34 (2003) 365–383.

[6] W. Paschen, T. Mengesdorf, Endoplasmic reticulum stress response and neurodegeneration, Cell Calcium 38 (2005) 409–415.

[7] W.X. Li, Y.Y. Deng, F. Li, Icariin, a major constituent of flavonoids from Epimedium brevicornum, protects against cognitive deficits induced by chronic brain hypoperfusion via its anti-amyloidogenic effect in rats, Pharmacol. Biochem. Behav. 138 (2015) 40–48.

[8] H. Nian, M.H. Ma, S.S. Nian, Antiosteoporotic activity of icariin in ovariectomized rats, Phytomedicine 16 (2009) 320–326.

[9] Y. Pan, L.D. Kong, Y.C. Li, Icariin from Epimedium brevicornum attenuates chronic mild stress-induced behavioral and neuroendocrinological alterations in male Wistar rats, Pharmacol. Biochem. Behav. 87 (2007) 130–140.

[10] J.H. Huang, W.J. Cai, X.M. Zhang, Icariin promotes self-renewal of neural stem cells: an involvement of extracellular regulated kinase signaling pathway, Chin. J. Integr. Med. 20 (2014) 107–115.

[11] H. Zhang, B. Liu, J. Wu, Icariin inhibits corticosterone-induced apoptosis in hypothalamic neurons via the PI3-K/Akt signaling pathway, Mol. Med. Rep. 6 (2012) 967–972.

[12] F. Li, Q.H. Gong, J.S. Shi, Icariin isolated from Epimedium brevicornum Maxim attenuates learning and memory deficits induced by d-galactose in rats, Pharmacol. Biochem. Behav. 96 (2010) 301–305.

[13] J. Guo, F. Li, J.S. Shi, Protective effects of icariin on brain dysfunction induced by lipopolysaccharide in rats, Phytomedicine 17 (2010) 950–955.

[14] T. Urano, C. Tohda, Icariin improves memory impairment in Alzheimer's disease model mice (5xFAD) and attenuates amyloid β-induced neurite atrophy, Phytother. Res. 24 (2010) 1658–1663.

[15] K.W. Zeng, H. Ko, H.O. Yang, Icariin attenuates β-amyloid-induced neurotoxicity by inhibition of tau protein hyperphosphorylation in PC12 cells, J. Neuro-Oncol. 59 (2010) 542–550.

[16] K.W. Zeng, H. Fu, G.X. Liu, Icariin attenuates lipopolysaccharide-induced microglial activation and resultant death of neurons by inhibiting TAK1/IKK/NF-κB and JNK/P38 MAPK pathways, Int. Immunopharmacol. 10 (2010) 668–678.

[17] C. Sheng, P. Xu, K. Zhou, Icariin attenuates synaptic and cognitive deficits in an $A\beta_{1\text{-}42}$-induced rat model of Alzheimer's disease, Biomed. Res. Int. 2017 (2017) 1–12.

[18] F. Li, H.X. Dong, Q.H. Gong, Icariin decreases both APP and Aβ levels and increases neurogenesis in the brain of Tg2576 mice, Neuroscience 304 (2015) 29–35.

[19] C. Angeloni, M.C. Barbalace, S. Hrelia, Icariin and its metabolites as potential protective phytochemicals against Alzheimer's disease, Front. Pharmacol. 10 (2019) 271.

[20] S. Salomone, F. Caraci, G.M. Leggio, New pharmacological strategies for treatment of Alzheimer's disease: focus on disease modifying drugs, Br. J. Clin. Pharmacol. 73 (2012) 504–517.

[21] F. Jin, Q.H. Gong, J.S. Shi, Icariin, a phosphodiesterase-5 inhibitor improves learning and memory in APP/PS1 transgenic mice by stimulation of NO/cGMP signalling, Int. J. Neuropsychopharmacol. 17 (2014) 871–881.

[22] I. Tabas, D. Ron, Integrating the mechanisms of apoptosis induced by endoplasmic reticulum stress, Nat. Cell Biol. 13 (2011) 184–190.

[23] H. Zinszner, M. Kuroda, X. Wang, CHOP is implicated in programmed cell death in response to impaired function of the endoplasmic reticulum, Genes Dev. 12 (1998) 982–995.

[24] X. Wang, W. Xia, K. Li, Rapamycin regulates cholesterol biosynthesis and cytoplasmic ribosomal proteins in hippocampus and temporal lobe of APP/PS1 mouse, J. Neurol. Sci. 399 (2019) 125–139.

[25] M. Yu, X. Chen, J. Liu, Gallic acid disruption of $A\beta_{1\text{–}42}$ aggregation rescues cognitive decline of APP/PS1 double transgenic mouse, Neurobiol. Dis. (2019) 67–80.

[26] Z. Cai, C. Wang, W. He, Berberine alleviates amyloid-beta pathology in the brain of APP/PS1 transgenic mice via inhibiting β/γ-secretases activity and enhancing α-secretases, Curr. Alzheimer Res. 15 (2018) 1045–1052.

[27] G. Joshi, K.A. Gan, D.A. Johnson, Increased Alzheimer's disease-like pathology in the APP/PS1dE9 mouse model lacking Nrf2 through modulation of autophagy, Neurobiol. Aging 36 (2015) 664–679.

[28] X.L. He, N. Yan, H. Zhang, Hydrogen sulfide improves spatial memory impairment and decreases production of Aβ in APP/PS1 transgenic mice, Neurochem. Int. 67 (2014) 1–8.

[29] L. Devi, M. Ohno, PERK mediates eIF2α phosphorylation responsible for BACE1 elevation, CREB dysfunction and neurodegeneration in a mouse model of Alzheimer's disease, Neurobiol. Aging 35 (2014) 2272–2281.

[30] Y. Du, J. Qu, W. Zhang, Morin reverses neuropathological and cognitive impairments in APPswe/PS1dE9 mice by targeting multiple pathogenic mechanisms, J, Neuropharmacology (2016) 1–13.

[31] Y. Liu, X. Zhu, Endoplasmic reticulum-mitochondria tethering in neurodegen-erative diseases, Transl. Neurodegener. 6 (2017) 21.

[32] W.B.P. Lucke, R.C. Turner, A.F. Logsdon, Endoplasmic reticulum stress implicated in chronic traumatic encephalopathy, J. Neurosurg. 124 (2016) 1–16.

[33] K.T. Pfaffenbach, M. Pong, T.E. Morgan, GRP78/BiP is a novel downstream target of IGF-1 receptor mediated signaling, J. Cell. Physiol. 227 (2012) 3803–3811.

[34] E. Szegezdi, S.E. Logue, A.M. Gorman, Mediators of endoplasmic reticulum stress-induced apoptosis. Mediators of endoplasmic reticulum stress-induced apoptosis, EMBO Rep. 7 (2006) 880–885.

[35] D. Ron, P. Walter, Signal integration in the endoplasmic reticulum unfolded protein response, Nat. Rev. Mol. Cell Biol. 8 (2007) 519–529.

[36] J.J. Hoozemans, E.S. van Haastert, D.A. Nijholt, The unfolded protein response is activated in pretangle neurons in Alzheimer's disease hippocampus, Am. J. Pathol. 174 (2009) 1241–1251.

[37] M.P. Mattson, Apoptosis in neurodegenerative disorders, Nat. Rev. Mol. Cell Biol. 1 (2000) 120–129.

[38] J. Hitomi, T. Katayama, Y. Eguchi, Involvement of caspase-4 in endoplasmic reticulum stress-induced apoptosis and A-induced cell death, J. Cell Biol. 165 (2014) 347–356.

[39] A.C.R.G. Fonseca, E. Ferreiro, C.R. Oliveira, Activation of the endoplasmic reticulum stress response by the $A\beta_{1\text{–}40}$ peptide in brain endothelial cells, Biochim. Biophys. Acta (BBA) - Mol. Basis Dis. 1832 (2013) 2191–2203.

[40] N. Louneva, J.W. Cohen, L.Y. Han, Caspase-3 is enriched in postsynaptic densities and increased in Alzheimer's disease, Am. J. Pathol. 173 (2014) 1488–1495.

[41] P.E. Czabotar, G. Lessene, A. Strasser, Control of apoptosis by the BCL-2 protein family: implications for physiology and therapy, Nat. Rev. Mol. Cell Biol. 15 (2014) 49–63.